

Mechanics of Old Faithful Geyser, Calistoga, California

M. L. Rudolph,¹ M. Manga,¹ S. Hurwitz,² M. Johnston,² L. Karlstrom,^{1,3} and C.-Y. Wang¹

Received 26 September 2012; revised 14 November 2012; accepted 19 November 2012; published 21 December 2012.

[1] In order to probe the subsurface dynamics associated with geyser eruptions, we measured ground deformation at Old Faithful Geyser of Calistoga, CA. We present a physical model in which recharge during the period preceding an eruption is driven by pressure differences relative to the aquifer supplying the geyser. The model predicts that pressure and ground deformation are characterized by an exponential function of time, consistent with our observations. The geyser's conduit is connected to a reservoir at a depth of at least 42 m, and pressure changes in the reservoir can produce the observed ground deformations through either a poroelastic or elastic mechanical model. **Citation:** Rudolph, M. L., M. Manga, S. Hurwitz, M. Johnston, L. Karlstrom, and C.-Y. Wang (2012), Mechanics of Old Faithful Geyser, Calistoga, California, *Geophys. Res. Lett.*, 39, L24308, doi:10.1029/2012GL054012.

1. Introduction

[2] Geysers are features that episodically discharge water and steam. There are only ~1000 such features on Earth, numbering far fewer than fumaroles and hot springs, features that continuously discharge steam and water, respectively. Geysers have attracted interest from geophysicists because of the improbability of circumstances necessary to achieve episodic discharge [Ingebritsen and Rojstaczer, 1996], their extreme sensitivity to the passage of seismic waves [e.g., Husen et al., 2004; Silver and Valette-Silver, 1992], climatic forcing [Hurwitz et al., 2008], and strains induced by solid earth tides [Rinehart, 1972] and for their potential as analogs to volcanic systems [Kieffer, 1984; Kedar et al., 1996].

[3] Despite significant interest, important aspects of the geyser process remain poorly understood. Eruptions involve decompression boiling of water initially close to the hydrostatic boiling curve, but opinions differ as to whether eruptions are triggered by a near-surface processes or by processes occurring deeper in the geyser system [Steinberg and Merzhanov, 1981; Dowden et al., 1991]. After erupting, a geyser's underground fracture network fills with water which could come from a single source [Ingebritsen and Rojstaczer, 1993, 1996] or multiple reservoirs of hot and cold fluid [Steinberg and Merzhanov, 1981]. The spatial and temporal evolution of pressure at depth during an eruption cycle depends on the processes that control recharge as well as the geometry and

transport properties of the medium that supplies the geyser. In turn, pressure changes at depth may produce observable ground deformations.

[4] We present the results of a field campaign at Old Faithful Geyser of Calistoga, CA (Figure 1), subsequently referred to as Calistoga Geyser. During the field campaign, we measured ground deformation with a borehole tiltmeter. We present a physical model to interpret the observed ground deformation during the period preceding an eruption. Our model predicts that recharge, and hence the interval between eruptions, is controlled by hydraulic transmissivity in a zone around the base of the geyser conduit and that eruptions initiate from a shallow (near-vent) process. The insights gained from our model may be applicable to some natural geysers and highlight the potential gains in understanding that we can expect from future multi-instrument field studies of natural geysers.

2. Field Observations

[5] Calistoga Geyser is an abandoned well, drilled in the late 1800 s to an unknown depth, which at the time of our study erupted with a period of 4.6 minutes. Calistoga Geyser has been monitored previously, and its interval between eruptions is sometimes bimodal and appears to be affected by seasonality and by distant earthquakes [Silver and Valette-Silver, 1992]. We carried out a multi-instrument geophysical study of Calistoga Geyser on May 6, 2010.

[6] We measured ground deformation using a Pinnacle 5000 series borehole tiltmeter (1 nR resolution and 10 degree range) installed at a depth of 1.17 m, 16.8 m from the geyser's vent (Figure 1). Figure 2 shows the radial tilt time series (filtered to remove diurnal and longer-period signals), as well as the stacked (Figure 2b) radial tilt record with standard deviations. Stacking was performed by identifying local minima in a smoothed tilt timeseries. The stack contains tilt records from 22 eruptions recorded between 19:14 and 22:13 (UTC) on May 6, 2010. The borehole tiltmeter was sampled once every 5 seconds.

[7] We captured water flowing through a weir (the only outlet from the geyser's pool) and weighed the water using a portable scale during one eruption cycle to provide estimates of discharge. The discharge measured using this technique was nearly constant at 0.68 ± 0.04 l/s. Discharge was also estimated using Manning's equation, $V = R^{2/3} S^{1/2} / n$ where V is mean velocity in m/s, R is the hydraulic radius, and S is the channel slope, with $n = 0.02$, yielding discharge of 0.75 l/s. Based on the discharge estimates, the volume erupted is $1.9\text{--}2.1 \times 10^{-1} \text{ m}^3$. Because the exit point of the geyser is higher than the water level in the pool, recharge by drainage back into the conduit cannot occur.

[8] Eruption timing was measured using an (IR) sensor manufactured by ElectroOptical Systems connected to a simple Keplerian telescope (aperture 25.4 mm, f-ratio 1). The IR sensor operates at wavelengths of 7–18 μ , with

¹Department of Earth and Planetary Science, University of California, Berkeley, California, USA.

²U.S. Geological Survey, Menlo Park, California, USA.

³Department of Geophysics, Stanford University, Palo Alto, California, USA.

Corresponding author: M. L. Rudolph, Department of Earth and Planetary Science, University of California, 307 McCone Hall, Rm. 4767, Berkeley, CA 94720, USA. (rudolph@berkeley.edu)



Figure 1. (a) Aerial photo (USGS 6-inch orthophoto) showing geyser and instrument locations. (b) Picture of Calistoga Geyser erupting, looking to the SE.

temporal sensitivity between DC and 10 Hz. The wavelength range 7–18 μ corresponds to blackbody spectrum peak wavelength for temperatures of 161–413 K. The sensor’s field of view (~ 0.1 radian, area 1.8 m² at the geyser vent location) was positioned just above the geyser outlet. The IR sensor was sampled once every 5 seconds.

[9] We filmed vent activity using an array of digital video cameras with 1080p resolution at 60 frames per second (fps) and with a FLIR A320 thermal imaging camera (320 \times 240 pixels, 30 fps). Video recordings of vent activity were used for Particle Image Velocimetry (PIV) using the OpenPIV (www.openpiv.net) software package. The maximum exit velocity measured using PIV was 10–20 m/s, consistent with the sound speed in water-steam mixtures at 1 bar with 0.1–1% steam by mass [Kieffer, 1977], with corresponding specific enthalpy in the range 420–440 kJ/kg [Wagner et al., 2000]. The infrared video indicated that boiling temperatures are reached at the geyser vent during the initial, liquid-dominated, phase of the eruption.

3. Physical Model

[10] We develop a physical model of the geyser motivated by the observational constraints, specifically 1) regular eruption interval, tilt pattern, and discharge and 2) decreasing rate of tilt leading up to eruption (Figure 2). We seek constraints on the size and location of the region in which pore pressure changes during an eruption cycle. Because we measured ground deformation at a single point, we assume homogenous, isotropic, and axisymmetric material properties and geometry.

[11] We model the geyser conduit as a cylinder of radius r and length d (Figure 3a). We assume based on distant observations and photographs that the internal diameter of the conduit ($2r$) is between 5 cm and 7.6 cm, though it may be somewhat narrower at depth owing to scale deposits. We assume that the conduit is connected at its base to a water-saturated porous medium. We use a pore pressure diffusion length scale $R = \sqrt{DT}$ to define a “reservoir” (Figure 3) where D is a hydraulic diffusivity and T is the interval between eruptions. The reservoir is the region in which pore pressure changes significantly during an eruption cycle. We assume that far from

the geyser conduit, pore pressure P_∞ is uniform. Water flows into the reservoir at a rate given by:

$$Q(t) = \frac{2\pi k \delta}{\mu} [P_\infty - P(t)] \quad (1)$$

where k is an effective permeability, μ is fluid viscosity (assumed constant), δ is reservoir thickness, and P_∞ and $P(t)$ are far-field and reservoir pressures, respectively. We assume a single fluid phase in the reservoir and surroundings. We note that the far-field pressure is not known and may, in general,

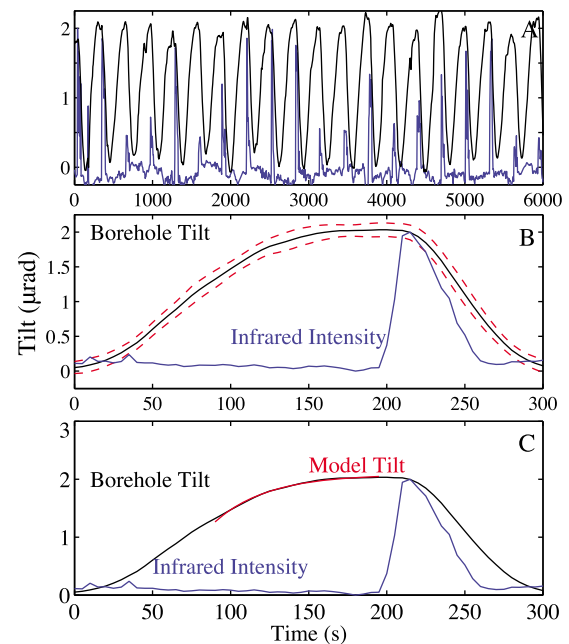


Figure 2. (a) Borehole tilt time series (black) and normalized single pixel infrared intensity (blue) for several eruptions beginning at 19:14:45 (UTC) on May 6, 2010. (b) Stacked borehole tilt record (black) and standard deviation (dashed red). Blue curve is stacked infrared intensity. (c) Same as Figure 2b but showing model fit (red) to tilt data (black).

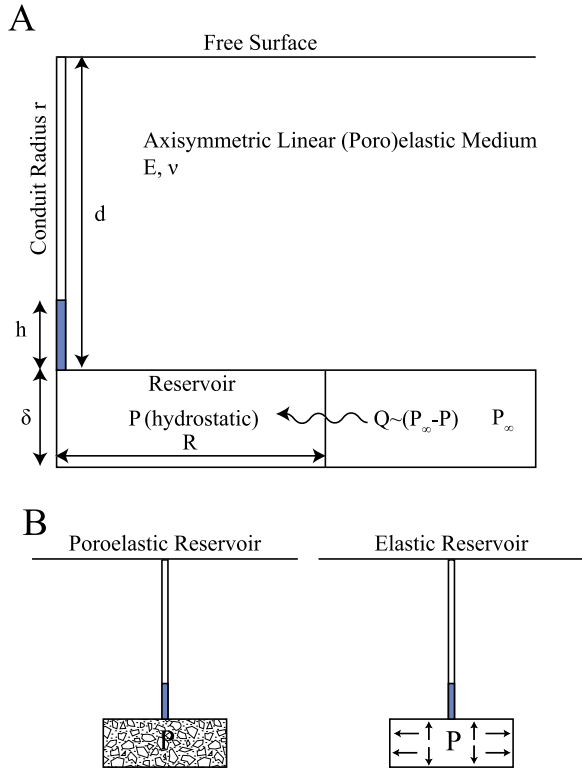


Figure 3. (a) Our conceptual model of Calistoga Geyser has three components: conduit, reservoir, and surroundings. The conduit fills during the interval between eruptions and the water at the base of the conduit is at the same pressure as the water in the reservoir. The far-field source of water has constant pressure and temperature. The surroundings are treated as a linear elastic medium that deforms in response to pressure changes in the reservoir. (b) The reservoir is modeled as either (left) part of a linear poroelastic medium or (right) as a cavity in an elastic medium.

be in excess of hydrostatic. Equation (1) can be viewed as a zero-dimensional version of the groundwater flow equation. We have adopted a zero-dimensional model because we do not know how pressure changes as a function of space and time during an eruption, a prerequisite to impose an initial condition when modeling the recharge phase. The pressure in the reservoir is assumed to be uniform and hydrostatic ($P(t) = \rho gh(t)$), where h is the conduit fill level (Figure 3a). The recharge rate into the reservoir Q is related to pressure P according to

$$dP/dt = \rho g Q / (\pi r^2), \quad (2)$$

where r is the conduit radius. We combine equations (1) and (2) to obtain the temporal evolution of reservoir pressure

$$P(t) = (P_0 - P_\infty) \exp\left(-\frac{2k\rho g \delta}{\mu r^2} t\right) + P_\infty \quad (3)$$

where P_0 is the pressure in the reservoir at time $t = 0$. The form of equation (3) is a common feature of geyser models in which recharge is driven by pressure differences [Steinberg and Merzhanov, 1981; Kedar et al., 1998].

[12] We model surface displacements resulting from pressure changes at depth using two models, chosen to be

analogous to different conceptual models for geysers in which the reservoir is assumed to be either a cavity [e.g., Steinberg and Merzhanov, 1981] or a porous medium [e.g., Ingebritsen and Rojstaczer, 1993], as illustrated in Figure 3b. The first model considers the possibility that the reservoir and its surroundings behave as an homogenous isotropic linear poroelastic material. Pressure changes in the reservoir (Figure 3a) produce volumetric strains and deform the surroundings elastically. In the second model, we assume that there is a cavity at depth, conceptually similar to a magma chamber, and pressure changes within the cavity cause the elastic surroundings to deform.

[13] The constitutive equation for the poroelastic model is

$$\sigma_{ij} = 2G\epsilon_{ij} + \frac{2G\nu}{1-2\nu}\epsilon_{ij}\delta_{ij} - \alpha p\delta_{ij} \quad (4)$$

where G (measured in Pa) and ν (dimensionless) are the shear modulus and Poisson's ratio and α is the Biot coefficient. We solve the momentum equation $\nabla \cdot \sigma = \underline{0}$ using an implementation of the finite element formulation described in Zienkiewicz and Taylor [2005, chapter 6]. We used bilinear rectangular elements for both displacement and pressure on a non-uniformly spaced grid. We assume for the sake of simplicity that $\alpha = 1.0$, which is equivalent to assuming that the solid phase is incompressible [Wang, 2000]. The domain has a free surface and we compute tilt (ψ) directly from the displacement field. We evaluate the computed tilt at the location x of the borehole tiltmeter and compare with the observed radial tilt. We note that in our model, tilt is linearly proportional to pressure change:

$$\psi(t) = k_\psi(\nu, \alpha, R, d, \delta, x) \frac{P(t)}{G} \quad (5)$$

where k_ψ is a coefficient relating changes in pressure to changes in tilt and R , d , δ are the effective reservoir radius, depth, and thickness. Values for the parameters are listed in Table 1. Laboratory values of the shear modulus G for sedimentary and volcanic rocks are typically in the range $0.4 \times 10^{10} - 4 \times 10^{10}$ Pa and Poisson's ratio ν is typically 0.2–0.25 [Turcotte and Schubert, 2002]. The effective value of the in-situ shear modulus may be at least an order of magnitude lower than the laboratory values [Davis, 1986]. The modeled tilt is inversely proportional to the shear modulus G .

[14] For the elastic model, we computed displacements using the axisymmetric program mode of FEAP v8.3 [Taylor, 2011]. As for the poroelastic model, both displacement and

Table 1. Summary of Parameters Entering the Mathematical Model

Parameter	Description	Value or Range Considered
r	Radius of geyser conduit	2.5–3.84 cm
d	Depth to reservoir	40–100 m
δ	Thickness of reservoir	0.5–10 m
R	Radius of reservoir	1–50 m
ρ	Fluid density	10^3 kg/m ³
G	Shear modulus	4×10^9 Pa
α	Biot coefficient	1.0
ν	Poisson's ratio	0.25

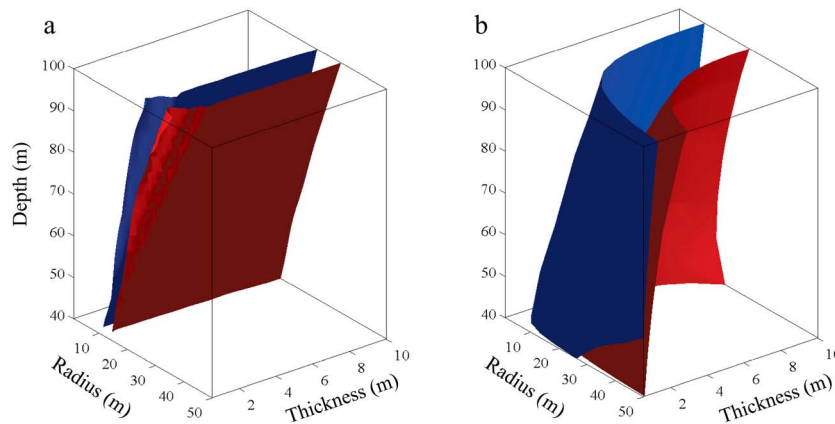


Figure 4. Isosurfaces of tilt coefficient k_ψ (equation (5)) calculated using (a) poroelastic and (b) elastic deformation source models (Section 3). Blue surface corresponds to $k_\psi = 2.1 \cdot 10^{-12}$ rad/Pa and red surface to $k_\psi = 1.4 \cdot 10^{-11}$ rad/Pa. k_ψ depends on tiltmeter position in addition to the quantities on the three axes shown, hence no axes can be eliminated through non-dimensionalization. The isosurfaces shown depend on E , ν , and α , with values given in Table 1.

tilt are linearly proportional to pressure change. The tilt-pressure coefficient k_ψ for the elastic case depends on the same variables as for the poroelastic case except for the absence of the Biot coefficient α .

[15] Equation (3) predicts that tilt during the recharge phase is described by an exponential function of time. We fit an exponential curve to the stacked borehole radial tilt record (90–195 s in Figure 2). The length of the temporal window used for curve fitting was chosen by maximizing the coefficient of determination R^2 while varying the starting point of the window between 0 s (the time of minimum tilt) and 195 s (the time of eruption onset inferred from the IR sensor). The exponential fit of the form $\psi(t) = k_\psi[(P_0 - P_\infty) \exp(-K_1 t) + P_\infty]$ allows us to directly constrain only the exponential decay constant $K_1 = 2k\rho g\delta/(\mu r^2)$ (best-fit value $2.95 \pm 0.2 \times 10^{-2} \text{ s}^{-1}$).

4. Discussion

[16] We can place some bounds on the range of permissible values of k_ψ and consequently on the range of the parameters R , d and δ that describe reservoir geometry. The removal of the volume erupted in a cycle (0.19 m^3) would lower the water level in the conduit by 42–97 m for the range of conduit radii considered. The corresponding pressure changes during an eruption cycle are $4.1 \times 10^5 - 9.5 \times 10^5$ Pa. The range of tilt during an eruption cycle is $2.0 \mu\text{rad}$, so the tilt coefficient k_ψ should have a value between 2.1×10^{-12} and 4.9×10^{-12} rad/Pa. We show isosurfaces for these values of the tilt pressure coefficient for both the poroelastic model and the elastic model in R , d , δ space in Figure 4. For any point lying between the blue and red isosurfaces in Figure 4, there exists a choice of the permeability k that will produce the observed tilt amplitude and exponential timescale. In other conceptual models of natural geysers, the component analogous to our reservoir is either a cavity [Steinberg and Merzhanov, 1981] or a porous medium [Ingebritsen and Rojstaczer, 1993]. Because we can explain the observed tilt signal using either type of reservoir, we cannot distinguish between these two possibilities, but future studies using additional tiltmeters may allow us to distinguish between these two end-member options.

[17] Despite the significant ambiguity in source location and transport properties, our model satisfies all of the available observational constraints. The surface deformations support a conceptual model for Calistoga geyser in which a vertical pipe is fed by recharge from a single hot liquid water reservoir at a rate that depends on the fill level in the pipe and the far-field pressure P_∞ . Seasonal variations in groundwater recharge may lead to changes in P_∞ , and hence affect the interval between eruptions [Silver and Valette-Silver, 1992]. In the model of the geyser process proposed by Steinberg and Merzhanov [1981], water is drawn from the hot source at a constant rate irrespective of the geyser’s chamber pressure whereas water is drawn from the cold reservoir at a rate proportional to the pressure difference between the cold water reservoir and the geyser chamber. If water flowed into Calistoga Geysers’ reservoir and conduit at a constant rate irrespective of fill level h , we would expect h , P , and ψ to vary linearly in time during the recharge phase. We see no evidence for such behavior. Based on the observed exit velocity and temperature, the fluid entering the base of the conduit has a specific enthalpy in excess of the boiling-curve enthalpy at atmospheric pressure. Hence, as the geyser’s fracture network is filled, the fluid in the upper portion of the conduit remains near the boiling curve and the removal of some overburden will lead to decompression boiling [Kieffer, 1989].

[18] **Acknowledgments.** This paper emerged in part from ideas discussed and measurements performed by students in EPS 200 at UC Berkeley in collaboration with USGS Menlo Park. Jennifer Frederick helped make the discharge measurements. Ben Andrews operated the video cameras. Edwin Kite operated the FLIR camera. Zack Geballe and Ian Rose mapped the instrument locations. Fred Murphy and Doug Myren assisted with instrumentation and data loggers. This work could not have been carried out without the generosity and support of the owners of Old Faithful Geyser of Calistoga, CA. Shaul Hurwitz and Malcolm Johnston were supported by the USGS Volcano Hazards and Earthquake Hazards programs, respectively. We thank Sharon Kedar and an anonymous reviewer for their comments. This work was supported in part by NSF grant EAR-1114184.

[19] The Editor thanks two anonymous reviewers for their assistance in evaluating this paper.

References

- Davis, P. M. (1986), Surface deformation due to inflation of an arbitrarily oriented triaxial ellipsoidal cavity in an elastic half-space, with reference to Kilauea Volcano, Hawaii, *J. Geophys. Res.*, *91*(B7), 7429–7438.

- Dowden, J., P. Kapadia, G. Brown, and H. Rymer (1991), Dynamics of a geyser eruption, *J. Geophys. Res.*, *96*, 18,059–18,071.
- Hurwitz, S., A. Kumar, R. Taylor, and H. Heasler (2008), Climate-induced variations of geyser periodicity in Yellowstone National Park, USA, *Geology*, *36*(6), 451–454.
- Husen, S., R. Taylor, R. Smith, and H. Heasler (2004), Changes in geyser eruption behavior and remotely triggered seismicity in Yellowstone National Park produced by the 2002 M 7.9 Denali fault earthquake, Alaska, *Geology*, *32*(6), 537–540.
- Ingebritsen, S. E., and S. A. Rojstaczer (1993), Controls on geyser periodicity, *Science*, *262*(5135), 889–892.
- Ingebritsen, S. E., and S. A. Rojstaczer (1996), Geyser periodicity and the response of geysers to deformation, *J. Geophys. Res.*, *101*, 21,891–21,906.
- Kedar, S., B. Sturtevant, and H. Kanamori (1996), The origin of harmonic tremor at Old Faithful Geyser, *Nature*, *379*, 708–711.
- Kedar, S., H. Kanamori, and B. Sturtevant (1998), Bubble collapse as the source of tremor at Old Faithful Geyser, *J. Geophys. Res.*, *103*, 24,283–24,300.
- Kieffer, S. W. (1977), Sound speed in liquid-gas mixtures: Water-air and water-steam, *J. Geophys. Res.*, *82*(20), 2895–2904.
- Kieffer, S. W. (1984), Seismicity at Old Faithful Geyser: An isolated source of geothermal noise and possible analogue of volcanic seismicity, *J. Volcanol. Geotherm. Res.*, *22*(1–2), 59–95.
- Kieffer, S. W. (1989), Geologic nozzles, *Rev. Geophys.*, *27*(1), 3–38.
- Rinehart, J. S. (1972), Fluctuations in geyser activity caused by variations in Earth tidal forces, barometric pressure, and tectonic stresses, *J. Geophys. Res.*, *77*(2), 342–350.
- Silver, P. G., and N. J. Valette-Silver (1992), Detection of hydrothermal precursors to large Northern California earthquakes, *Science*, *257*(5075), 1363–1368.
- Steinberg, G., and A. Merzhanov (1981), Geyser process: Its theory, modeling, and field experiment. Part 1. Theory of the geyser process, *Mod. Geol.*, *8*, 67–70.
- Taylor, R. L. (2011), *FEAP: A Finite Element Analysis Program*, Univ. of Calif., Berkeley.
- Turcotte, D. L., and G. Schubert (2002), *Geodynamics*, 2nd ed., Cambridge Univ. Press, New York.
- Wagner, W., et al. (2000), The IAPWS Industrial Formulation 1997 for the thermodynamic properties of water and steam, *J. Eng. Gas Turbines Power*, *122*(1), 150–184.
- Wang, H. (2000), *Theory of Linear Poroelasticity With Applications to Geomechanics and Hydrogeology*, Princeton Univ. Press, Princeton, N. J.
- Zienkiewicz, O., and R. Taylor (2005), *The Finite Element Method: Its Basis and Fundamentals*, 6th ed., Elsevier Butterworth-Heinemann, Amsterdam.